J Mater Sci: Mater Electron (2013) 24:1341–1347
DOI 10.1007/s10854-012-0931-2

Hysteresis loops of MgB_2 + Co composite tapes

E. Altin · D. M. Gokhfeld · S. V. Komogortsev · S. Altin · M. E. Yakinci

Received: 29 August 2012 / Accepted: 1 October 2012 / Published online: 18 October 2012

Abstract The $(MgB_2)_{1-x}Co_x$ composite tapes fabricated by the ex situ PIT method were investigated. The structural and magnetic properties were characterized. Only MgB_2 and Co phases were observed in the composites while $x \leq 0.2$. A superconducting transition temperature was stable for these samples. Enhancement of the critical current density is found for $x = 0.1$.

1 Introduction

Since the discovery of superconductivity on MgB_2 with a critical temperature of 39 K [1], many studies have been made to increase the ability of MgB_2 to sustain superconductivity at high magnetic fields with a high current density. The critical current density, which is related to pinning of Abrikosov vortices, can be enhanced by formation of structural defects acting as pinning centers. Composites including a superconductor and non-superconducting ingredients are prepared to increase the pinning [2–7]. However non-superconducting additions may penetrate in the MgB_2 lattice and decrease the superconductor transition temperature. Much attention has been focused on magnetic particles in superconducting matrix [8–14]. It is supposed that the increase of magnetization hysteresis in superconducting materials may be greater for magnetic inclusions than for non-magnetic ones. It is due to the flux interaction with magnetic impurities in superconducting materials [10]. Also there is fundamental interest to study interplay of superconductivity and magnetism in such composites where the ferromagnetic component influences ambiguously on superconducting properties.

Co is good candidate for the ferromagnetic component of the composite with MgB_2 because it is chemically stable enough and has high Curie temperature and a saturation magnetization. There were several studies on the MgB_2 + Co composites early [15–19]. Unfortunately the superconducting transition temperature decreases as Co content increases. Also, high Co adding in MgB_2 may result in formation of the amorphous CoB phase in the samples [15–17]. Pinning enhancement was not found in these MgB_2 + Co composite, on the contrary Co addition was found to weaken pinning in MgB_2 [17, 18].

In this study, we successfully synthesized the MgB_2 + Co composite tapes with different Co content by the powder-in-tube (PIT) method and characterized their structure and magnetic properties.

2 Experimental section

The composite tapes with nominal composition of $(MgB_2)_{1-x}Co_x$ ($x = 0.0$, 0.005, 0.01, 0.03, 0.05, 0.07, 0.1, 0.2, 0.3 and 0.4) were fabricated using ex situ PIT method. High purity commercial MgB_2 (Alfa Aesar Co.) and Co powders were mixed in the agate mortar for 10 h under Ar atmosphere. The mixed powders were tightly filled into silver tube of 1–3 cm length, 5 mm inner and 5.5 mm outer diameters under Ar atmosphere. The Ag-tubes with filled

E. Altin
Bilimsel ve Teknolojik Araştırma Merkezi, Inonu Universitesi, 44280 Malatya, Turkey

D. M. Gokhfeld · S. V. Komogortsev
L.V. Kirensky Institute of Physics SB RAS, Akademgorodok 50/38, 660036 Krasnoyarsk, Russia

S. Altin (✉) · M. E. Yakinci
Fen Edebiyat Fakultesi Fizik Bolumu, Superiletkenlik Arastirma Grubu, Inonu Universitesi, 44280 Malatya, Turkey
e-mail: serdar.altin@inonu.edu.tr

powders were cold-pressed under a loading of 8 tons and rolled to obtain the tapes with the thickness of 0.4 mm and the width of about 5 mm. The tapes were heat treated at 630 °C for 24 h with a heating/cooling rate as 10 °C/min under Ar atmosphere. Rigaku RadB X-ray diffractometer with Cu K_α radiation ($\lambda = 1.5405$ Å) was used to characterize the structure of all the samples. The scan speed of 2° per min in the range of 3°–80° was selected during the measurements. The microstructure of the tapes was investigated by using scanning electron microscopy (SEM) with Leo Evo-40 VP scanning electron microscope. DC magnetization and magnetic hysteresis measurements were performed by Cryogenic Q-3398 vibrating sample magnetometer. The superconducting transition temperature of the tapes was defined as the temperature at which a diamagnetic signal appears on $M(T)$. In the magnetic hysteresis experiments, the measurements were carried out at three different temperatures (10, 20 and 30 K) and magnetic field up to 7 T.

3 Results and discussion

Figure 1 shows a typical X-ray diffraction (XRD) pattern of $(MgB_2)_{1-x}Co_x$ composite at room temperature. All the intense peaks can be indexed assuming a hexagonal unit cell of MgB_2 with lattice parameters listed in Table 1. Williamson−Hall method [20] was used to estimate the average size and the strain of MgB_2 crystallites (Table 1). The average crystallite size is about 40 nm in all samples. The nanocrystalline nature of investigated MgB_2 may be the reason of slightly enhanced lattice parameters in comparison with literature data [21]. The MgB_2 lattice parameters of composites are constant both for the pure MgB_2 and for composite tapes with different Co fraction.

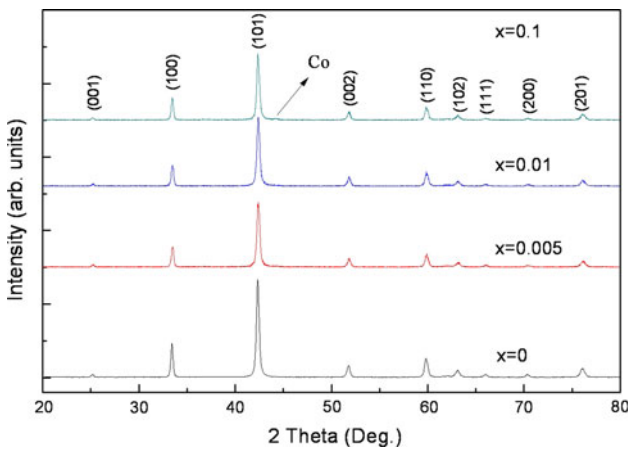

Fig. 1 XRD patterns of the $(MgB_2)_{1-x}Co_x$ tapes

Table 1 Cell parameters, crystallite size D and internal deformations ε in $(MgB_2)_{1-x}Co_x$

x	a (Å)	c (Å)	D (nm)	ε (%)
0	3.090 ± 0.003	3.532 ± 0.004	36 ± 5	0.24 ± 0.03
0.005	3.086 ± 0.002	3.526 ± 0.002	39 ± 6	0.28 ± 0.02
0.01	3.087 ± 0.003	3.527 ± 0.003	39 ± 5	0.28 ± 0.02
0.1	3.088 ± 0.002	3.529 ± 0.004	39 ± 5	0.26 ± 0.02

It implies that the Co atoms do not penetrate in the MgB_2 lattice.

At XRD pattern for the sample with $x = 0.1$ the reflex near 44.2° is referred to Co particles with the fcc lattice [22]. Realization of the fcc lattice means that the size of the Co particles should be ≤20 nm, because this structure is unstable for larger Co particles [23].

Scanning electronic microscopy (SEM) images of the samples with $x = 0$, 0.005, 0.01 and 0.1 are presented in Fig. 2. The sample with $x = 0$ is composed of pure MgB_2 grains with sizes distributed from ~0.1 to 2 μm and an average size ~1 μm. Also some porosity is observed. The samples with $x = 0.005$, 0.01 and 0.1 have similar SEM images. White regions indicating Co are spreading in the sample with increasing Co content. These samples have some smaller MgB_2 grain size and higher porosity.

The XRD and SEM data result that Co atoms aggregated at nano-sized particles covering the MgB_2 grains.

Temperature evolution of the magnetization is presented on Fig. 3. The superconducting transition temperature of 39.0 ± 0.3 K was obtained for all samples with $x \leq 0.2$. Decrease of the superconducting transition temperature is observed for the samples with $x \geq 0.3$. Magnetization loops of $(MgB_2)_{1-x}Co_x$ composite tapes are presented in Fig. 4 for $x = 0$, 0.05 and 0.1 at $T = 10$, 20 and 30 K and for $x = 0.2$, 0.3 and 0.4 at 30 K. As seen, the $M(H)$ curves of the composite tapes are formed by superconducting M_{SC} and ferromagnetic M_{FM} contributions. Saturation and coercivity are regulated by shares of M_{SC} and M_{FM}. Let us express the net magnetization of the tapes as $M(H) = (1\_x_m)\ M_{SC}(H) + x_m\ M_{FM}(H)$, where x_m is the mass fraction of Co for M in emu/g units. We expected that a Co addition modifies the $M_{SC}(H)$ dependence in comparison with the $M(H)$ loop of the pure MgB_2 tape. To verify this suggestion the ferromagnetic contribution were analyzed firstly, and then we have extracted $M_{SC}(H)$ dependencies of the tapes.

The $M(H)$ curves of the tapes at high H are determined by only the Co particles magnetization because the magnetization of the MgB_2 grains at $H > 4$ T was nearly zero. Approach to saturation of ferromagnetic particles is described by [24]:

$$M_{FM}(H) = Ms(1 - 1/15(H_a/H)^2) + \xi H, \quad (1)$$

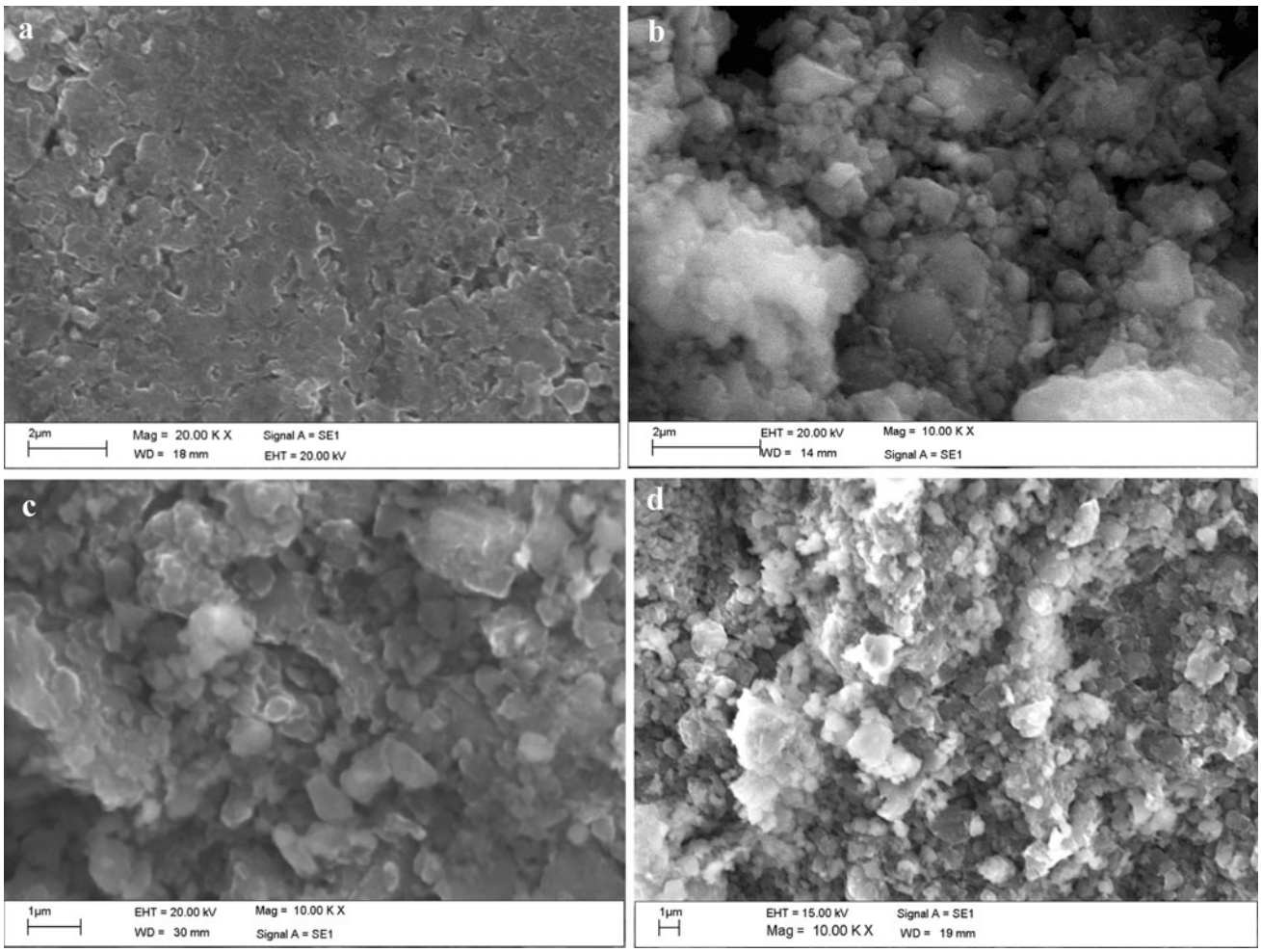

Fig. 2 SEM images of the $(MgB_2)_{1-x}Co_x$ system for **a** $x = 0$, **b** $x = 0.005$, **c** $x = 0.01$, **d** $x = 0.1$

where M_s is the saturation magnetization, H_a is the field of the local magnetic anisotropy, ξ is the paramagnetic susceptibility. Expression (1) fits successfully the high field parts of the $M(H)$ curves at range 1–6 T (see Fig. 4 for the samples with $x = 0.2$, 0.3, 0.4 at $T = 30$ K). The fitting parameter H_a is about 0.9 T for these samples that is the same as H_a of Co nanoparticles with the fcc lattice dispersed in the amorphous carbon [24].

Figure 5 demonstrates the saturation magnetization M_s of the Co particles estimated from the magnetization of the $(MgB_2)_{1-x}Co_x$ composite tapes at $H = 7$ T. To obtain M_s of the Co particles a small paramagnetic magnetization of the pure MgB_2 tape at 7 T is subtracted from the magnetization of the composite tape. Obtained values of magnetization are reduced to the mass of Co in the composite. For the samples with $x > 0.1$, the values of M_s are close to the spontaneous magnetization of Co (160 emu/g). As x decreases to 0.005, M_s decreases to 120 emu/g. Decrease of the saturation magnetization for small x may be due to presence of isolated Co nanoparticles. The smallest isolated nano-sized Co particles would be superparamagnetic and their contribution in magnetization is negligible at 7 T. Also the M_s value may be reduced by the interface between Co and MgB_2 as its specific fraction increases with the Co content decreases. Observed decrease of the M_s value implies that there is no significant penetration of Mg or B atoms to the fcc Co lattice. The magnetization of fcc Co-X solid solutions decreases linearly with gradient ~ 5 emu/g per at.% [25, 26]. So the total concentration of Mg and B in our Co particles is below 10 %). This means that the shape of the $M_{FM}(H)$ dependence is the same for all investigated composite tapes. The $M_{FM}(H)$ loop obtained is characterized by next parameters: the coercive field $H_{coer} \approx 400$ Oe, the remnant magnetization $M_r \approx 0.13\ M_s$. The absence of mutual chemical penetration of Co and MgB_2 in our composites and the constant shape of $M_{FM}(H)$ loop allow to extract $M_{SC}(H)$ contribution as $M_{SC}(H) = (M(H) - x_m M_{FM}(H))/(1 - x_m)$.

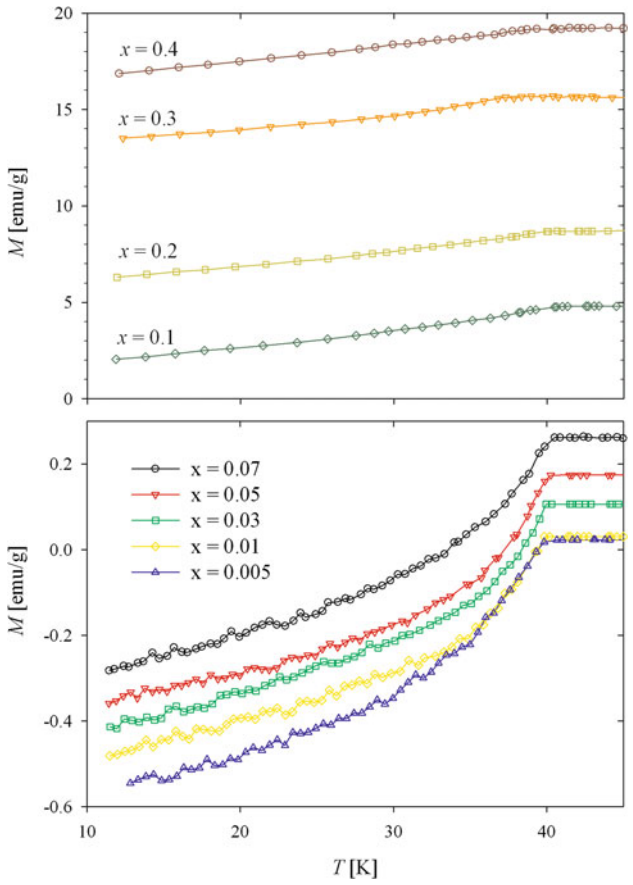

Fig. 3 Temperature dependence of magnetization of the $(MgB_2)_{1-x}Co_x$ tapes at $H = 0.1$ T

Figure 6 shows the extracted $M_{SC}(H)$ loops of the composite tapes and the $M(H)$ loops of the sample with $x = 0$. It appeared problematic to extract $M_{SC}(H)$ for the tapes with $x = 0.3$ and 0.4 because the $M_{SC}(H)$ response is indistinguishable in comparing to the M_{FM} contribution where. The non-symmetric hysteresis with respect to the $M = 0$ axis was obtained for the composite tapes. The width of the $M(H)$ loop of the sample with $x = 0$ is larger in 1.5 times and its asymmetry with respect to the $M = 0$ axis is smaller than those of the $M_{SC}(H)$ loops of the composite tapes at 10 K. All extracted $M_{SC}(H)$ dependencies are nearly coinciding with each other at $T = 10$ K. At higher temperatures this coincidence keeps only for the tapes with $x < 0.1$. At $T = 20$ K the $M_{SC}(H)$ loops of the samples with $x = 0.1$ and 0.2 become wider than the $M_{SC}(H)$ loops of other composite tapes. The $M_+(H)$ curves of samples with $x = 0.1$ and 0.2 coincides with $M_+(H)$ of other composite tapes at 10–30 K, here $M_+(H)$ is the branch of $M_{SC}(H)$ dependence for decreasing H. At the same time the $M_-(H)$ curves, which are the branch of $M_{SC}(H)$ dependence for increasing H, are near coincident at 20 K for the pure MgB_2 tape and for the samples with $x = 0.1$ and 0.2. At $T = 30$ K the $M_-(H)$ branches of the samples with $x = 0.1$ and 0.2 are situated lower than $M_-(H)$ of the tape with $x = 0$. Increase of diamagnetic response of the MgB_2 grains in the tapes with $x = 0.1$ and 0.2 is probably referred to magnetic percolation in the system of Co particles [27].

The critical current density J_c of the samples were calculated using Bean formula:

$$J_c = 30\frac{\Delta M}{2R}, \tag{2}$$

where $\Delta M = M_+ - M_-$ is the magnetization width measured in emu/cm^3 and $2R$ (in centimeters) corresponds to a characteristic structural scale which may be a size of crystallite, grain or sample. Magnitude of J_c is mainly determined by choice a working scale [28]. Table 2 gives the zero field J_c, J_{c0}, of the tape with $x = 0$ estimated for different $2R$ scales and the MgB_2 density $\rho = 2.57$ g/cm^3 at $T = 10$ K. The values of J_{c0} obtained by using the size of the crystallite and the sample look correspondingly overestimated and underestimated.

To make specified estimation of $2R$ we analyzed an asymmetry of the magnetization loops with respect to the $M = 0$ axis. The extended critical state model [29] was applied to fit the $M_{SC}(H)$ loops. Two fitting parameters are used in the model [29]: $\alpha_1 = j_cR$, determining the width of a magnetization loop, and $\alpha_2 = l_s/R$, determining its asymmetry. Here j_c is the maximal local critical current density, l_s is the depth of an equilibrium surface layer, and R is the radius of circulation of a screening supercurrent. It is supported [29] that l_s is about the London penetration depth, which is 48 nm for the higher gap of MgB_2 [30]. The value of α_2 was estimated to determine $2R$. Solid lines on Fig. 6 were computed with α_2 increasing from 0.08 at 10 K to 0.1 at 30 K for the pure MgB_2 tape and from 0.18 at 10 K to 0.2 at 30 K for the composite MgB_2 tapes with $x \leq 0.1$. Successful fitting of the $M_{SC}(H)$ loops confirms that temperature evolution of pinning in MgB_2 grains is similar to one in BSCCO [29, 31]. At the same temperature range α_2 keep to be equal to 0.18 for the $M_{SC}(H)$ loops of the composite tapes with $x = 0.1$ and 0.2 such that the pinning is weakly affected by the temperature in this tapes.

Given $\alpha_2 = 0.08$, $2R$ is appeared to be equal to 1.2×10^{-4} cm that is about the average grain size of 1 mkm estimated from SEM images. Therefore the grain size is a key scale for magnetization of the investigated tapes. Figure 7 demonstrates the intragrain critical current density of the tapes estimated at $H = 0$, using $2R = 1$ μm. The pure MgB_2 tape has the $J_{c0} = 3.4\times10^7$ A/cm^2 that is comparable with the best magnetic J_{c0} of MgB_2 [2]. The composite tape with $x = 0.1$ has a smaller value of J_{c0} at 10 K, $J_{c0} = 2.2\times10^7$ A/cm^2. But influence of temperature

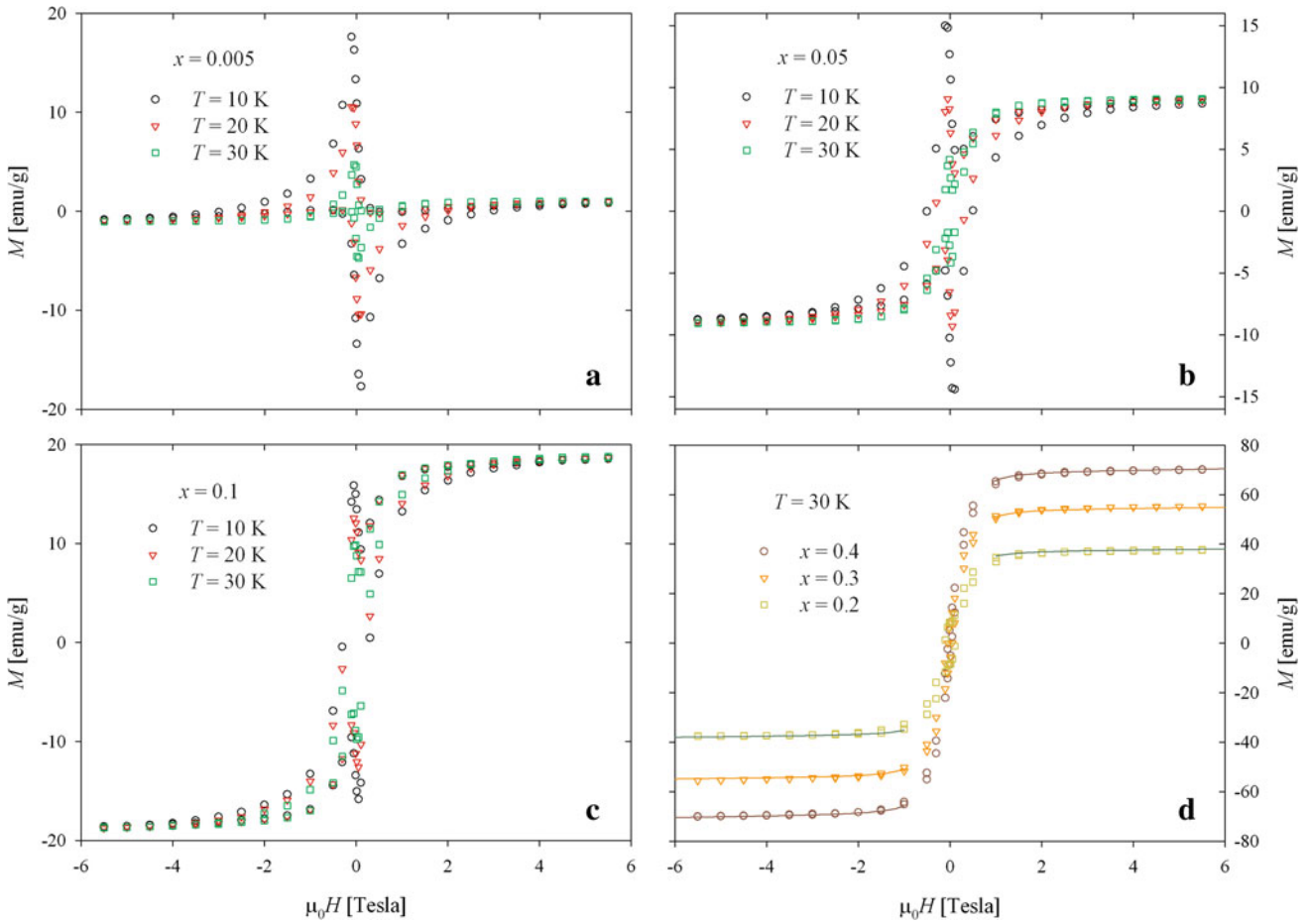

Fig. 4 Magnetization loops of the $(MgB_2)_{1-x}Co_x$ tapes. *Solid lines* are fitting curves computed by (1)

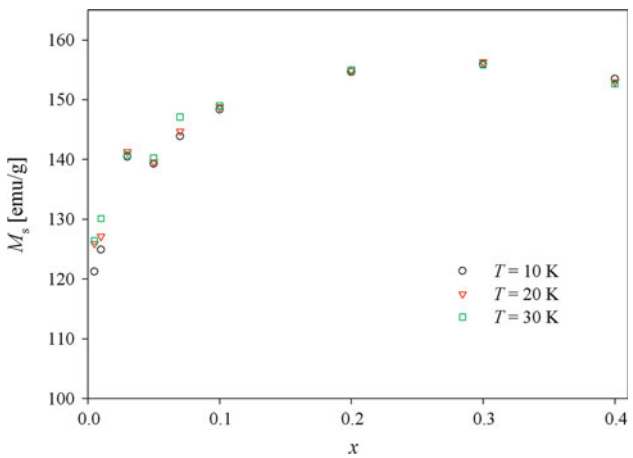

Fig. 5 Saturation magnetization M_s of the Co particles in the $(MgB_2)_{1-x}Co_x$ tapes

and magnetic field on J_c in the MgB_2 + Co tapes with $x = 0.1$ and 0.2 is observed to be weaker than in the tapes with $x < 0.1$. The tape with $x = 0.1$ has $J_{c0} = 1.32\times10^7$ A/cm^2 at $T = 30$ K which is larger than $J_{c0} = 1.09\times10^7$ A/cm^2 in the pure MgB_2 tape. At higher field pinning differs more noticeably, e.g. at $H = 1$ T, $J_c = 1.6\times10^6$ A/cm^2 at 30 K compared to 1.95×10^5 A/cm^2 in the pure MgB_2 tape.

The composite tapes have the smaller width of the $M_{SC}(H)$ loops at 10 K than the pure MgB_2 tape. It may be caused by next reasons: (1) Magnetic moment of ferromagnetic particles is expected to suppress superconductivity [32]. In this case the decreasing of the $M_{SC}(H)$ loop width must correlate with the value of Co fraction. However we found that the $M_{SC}(H)$ loops are nearly the same for different $x < 0.1$. Simple estimation of the internal field produced by the ferromagnetic component is given by $H_{in} = H - N\times M_s\times x$, where H_{in} is the internal field, N is demagnetization factor, $M_s = 1{,}445$ emu/cm^3 for Co. Given composites are macroscopically isotropic, $N = 4/3\pi$. For $x = 0.1$ we found $H_{in} = 0.06$ T that is negligible at high fields. Superconductivity is remarkable suppressed in the tapes with $x > 0.2$. (2) The porosity of the sample and the average size

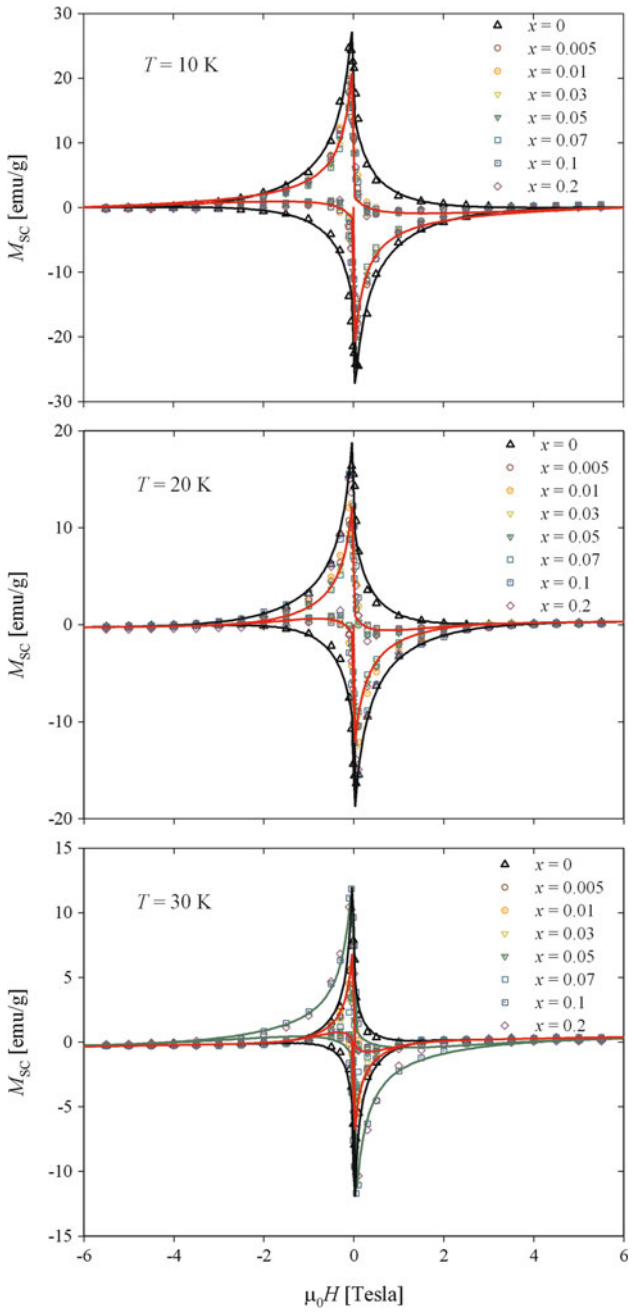

Fig. 6 Magnetization of the superconducting component. *Solid lines* are fitting curves of the extended critical state model

Table 2 Estimations of the critical current density of the MgB_2 tape at $T = 10$ K for different scales of the supercurrent circulation, $2R$

Structural scale	$2R$ [cm]	J_{c0} [A/cm^2]
crystallite	4×10^{-6}	8.5×10^{8}
grain	1×10^{-4}	3.4×10^{7}
sample	0.5	6.8×10^{3}

of superconducting grains may differ for the virgin MgB_2 tape and the composite tape. Porosity does not decrease the absolute values of magnetization in emu/g units. It follows

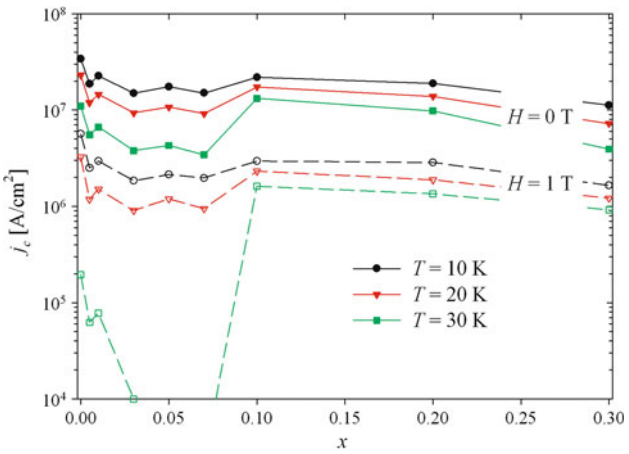

Fig. 7 Critical current density of the $(MgB_2)_{1-x}Co_x$ tapes at $H = 0$ (*full symbols*, *solid connecting lines*) and $H = 1$ T (*empty symbols*, *dotted connecting lines*)

that only some decreasing of grains during the composite tape preparation may only explain the smaller width of the $M_{SC}(H)$ loops.

We support that to improve the critical current the nano-sized Co particles should be distributed on the surface of superconducting grains. Combination of surface magnetic pinning particles and volume pinning centers is promising perspective for applied superconductors.

4 Conclusions

The $(MgB_2)_{1-x}Co_x$ tapes were synthesized by PIT technique. Characterization of structure and magnetic properties at temperatures of 10–30 K were performed. The Co nanoparticles spread in the composite and their saturation magnetization increases and approaches to 160 emu/g as Co content increased. An interpenetration of Co and MgB_2 in the tapes and a decrease in transition temperature were avoided for $x \leq 0.2$.

The magnetization loops of the composite tapes were considered as sum of superconducting M_{SC} and ferromagnetic M_{FM} components. The extended critical state model was used to analyze the asymmetric magnetization loops and choose the scale of the supercurrent circulation. It was observed that the critical current density of the composite tapes does not depend on x for small addition of Co ($x < 0.1$). Maximum of critical current density in the MgB_2 + Co tapes is found for $x = 0.1$ (2.2×10^7 A/cm^2 at $H = 0$, $T = 10$ K). For the tapes with $x \geq 0.3$ the critical current density falls down.

Acknowledgments The work is partly supported by project No. 20 of RAS program "Quantum mesoscopic and disordered structures" and grant No. 11-02-98007-p of Russian foundation for basic research.

References

1. J. Nagamatsu, N. Nakagawa, T. Muranaka, Y. Zenitani, J. Akimitsu, Nature **410**, 63 (2001)
2. C. Buzea, T. Yamashita, Supercond. Sci. Technol. **14**, R115 (2001)
3. S.X. Dou, A.V. Pan, S. Zhou, M. Ionescu, X.L. Wang, J. Horvat, H.K. Liu, P.R. Munroe, J. Appl. Phys. **94**, 1850 (2003)
4. M. Eisterer, Supercond. Sci. Technol. **20**, R47 (2007)
5. X.F. Pan, T.M. Shen, G. Li, C.H. Cheng, Y. Zhao, Phys. Stat. Solid. A **204**, 1555 (2007)
6. N. Ojha, G.D. Varma, H.K. Singh, V.P.S. Awana, J. Appl. Phys. **105**(07), E315 (2009)
7. C. Yao, X. Zhang, D. Wang, Z. Gao, L. Wang, Y. Qi, C. Wang, Y. Ma, S. Awaji, K. Watanabe, Supercond. Sci. Technol. **24**, 055016 (2011)
8. T.H. Alden, J.D. Livingston, J. Appl. Phys. **37**, 3551 (1966)
9. C.C. Koch, G.R. Love, J. Appl. Phys. **40**, 3582 (1969)
10. A. Snezhko, T. Prozorov, R. Prozorov, Phys. Rev. B **71**, 024527 (2005)
11. C. Cheng, Y. Zhao, Appl. Phys. Lett. **89**, 252501 (2006)
12. K.Q. Ruan, Z.M. Lv, H.Y. Wu, S.L. Huang, M. Li, Z.Q. Pang, Q.Y. Wang, Y. Feng, G. Yan, J. Supercond. Nov. Magn. **21**, 237 (2008)
13. T. Kuroda, T. Nakane, H. Kumukura, Phys C **469**, 9 (2009)
14. E. Taylan Koparan, A. Surdu, A. Sidorenko, E. Yanmaz, Phys. C. **473**, 1 (2012)
15. M. Kühberger, G. Gritzner, Phys. C. **370**, 39 (2002)
16. E. Kuzmann, Z. Homonnay, Z. Klencsar, M. Kühberger, A. Vertes, G. Gritzner, Supercond. Sci. Technol. **15**, 1479 (2002)
17. M.A. Aksan, M.E. Yakinci, A. Guldeste, J. Alloy. Compd. **424**, 33 (2006)
18. P.N. Togoulev, N.M. Suleimanov, K. Conder, Physica C **450**, 45 (2006)
19. S. Treiber, B. Stuhlofer, H.-U. Habermeier, J. Albrecht, Supercond. Sci. Technol. **22**, 045007 (2009)
20. G.K. Williamson, W. Hall, Acta Metall. **1**, 22 (1953)
21. M. Jones, R. Marsh, J. Am. Chem. Soc. **76**, 1434 (1954)
22. Natl. Bur. Stand. (U.S.) Monogr. **25** (1966) 10
23. O. Kitakami, H. Sato, Y. Shimada, F. Sato, M. Tanaka, Phys. Rev. B **56**, 13849 (1997)
24. S.V. Komogortsev, R.S. Iskhakov, ChN Barnakov, N.A. Momot, V.K. Maltsev, A.P. Kozlov, Phys. Met. Metallogr. **109**, 130 (2010)
25. R.S. Iskhakov, M.M. Brushtunov, I.A. Turpanov, Fiz. Met. Metalloved. **66**, 469 (1988)
26. K. Huller, G. Dietz, R. Hausmann, K. Kolpin, J. Magn. Magn. Mater. **53**, 103 (1985)
27. X. Batlle, V. Franco, A. Labarta, J. Appl. Phys. **88**, 1576 (2000)
28. J. Horvat, S. Soltanian, A.V. Pan, X.L. Wang, J. Appl. Phys. **96**, 4342 (2004)
29. D.M. Gokhfeld, D.A. Balaev, M.I. Petrov, S.I. Popkov, K.A. Shaykhutdinov, V.V. Valkov, J. Appl. Phys. **109**, 033904 (2011)
30. V. Moshchalkov, M. Menghini, T. Nishio, Q.H. Chen, A.V. Silhanek, V.H. Dao, L.F. Chibotaru, N.D. Zhigadlo, J. Karpinski, Phys. Rev. Lett. **102**, 117001 (2009)
31. S. Altin, D.M. Gokhfeld, Phys C **471**, 217 (2011)
32. K.A. Shaikhutdinov, D.A. Balaev, S.I. Popkov, M.I. Petrov, Phys. Solid State **45**, 1866 (2003)